Transition from Metastability to Instability in a Binary-Liquid Mixture

Hajime Tanaka
Department of Applied Physics and Applied Mechanics, Institute of Industrial Science, University of Tokyo, Minato-ku, Tokyo 106, Japan

Takeshi Yokokawa, Hajime Abe, Takafumi Hayashi, and Toshio Nishi
Department of Applied Physics, Faculty of Engineering, University of Tokyo, Bunkyo-ku, Tokyo 113, Japan
(Received 23 May 1990)

In a binary mixture of oligomers of styrene and ϵ-caprolactone, we have studied a transition from metastability to instability by changing a quench depth systematically under an off-critical quench condition. The concentration distribution function turns out to be a good fingerprint for determining whether phase separation is nucleation-growth type or spinodal-decomposition type. We also demonstrate clear *morphological and kinetic* evidence of a *diffuse* metastable-unstable transition or crossover phenomena theoretically predicted for the system with a finite-range interaction.

PACS numbers: 64.60.Ht, 61.41.+e, 64.70.Ja

Phase-separation phenomena in systems with a phase diagram have been intensively studied by many researchers.[1,2] It is widely known that the nucleation-growth (NG) type of phase separation occurs in the metastable region because of the existence of a barrier for nucleation, while the spinodal-decomposition (SD) type of phase separation occurs in the unstable region where fluctuations can grow without any barrier. Recent theoretical studies[3-5] show that the transition from metastability to instability may be diffuse in a short-range-force system and it is sharp only in a mean-field-like system.

The ideal limit of metastability is the locus of points where the free-energy barrier ΔF^* passes through of the order of a few k_BT. According to homogeneous nucleation theory, for $\delta\phi \equiv \phi_{ms} - \phi_{coex}^{(1)} \ll \phi_{coex}^{(2)} - \phi_{coex}^{(1)}$, where $\phi_{coex}^{(1)}$ and $\phi_{coex}^{(2)}$ are the two branches of the coexistence curve (see Fig. 1), the creation of a d-dimensional spherical droplet out of a metastable phase at concentration ϕ_{ms} involves a free energy[4]

$$\Delta F^* = \left[\frac{S_d}{d}\right]\left[\frac{d-1}{V_d}\right]^{d-1} \frac{f_{int}^d \chi_{coex}^{d-1}}{[\phi_{coex}^{(2)} - \phi_{coex}^{(1)}]^{2(d-1)}} \times \left[\frac{\delta\phi}{\phi_{coex}^{(2)} - \phi_{coex}^{(1)}}\right]^{-(d-1)},$$

where χ_{coex} is the susceptibility at the coexistence curve, S_d and V_d are the surface and volume of a d-dimensional unit sphere, and f_{int} is the interfacial free energy between two coexisting bulk phases at concentrations $\phi_{coex}^{(1)}$ and $\phi_{coex}^{(2)}$. The Ginzburg criterion tells us that for $r^d(1-T/T_c)^{(4-d)/2} \gg 1$ (T_c is the critical point, r is the interaction range) mean-field critical behavior occurs. A simple calculation shows that there exists a clear transition from nucleation to spinodal decomposition.[4,5] On the other hand, for $r^d(1-T/T_c)^{(4-d)/2} < 1$ non-mean-field critical behavior occurs, and $\Delta F^*/k_BT$ becomes of order unity long before the spinodal is reached. In this case a gradual transition from nucleation to spinodal decomposition occurs. The broadness of the transition is closely related to the range of the bare interaction.

The problem has been studied mainly from the theoretical viewpoint.[3-9] There have been few systematic, experimental studies on the transition from metastability to instability, though there have been several interesting studies[10-16] on nucleation itself. Here we study the transition in pattern formation from metastability to instability in a viscous liquid mixture. We have chosen an oligomer mixture since the viscosity is suitable for studying the phase-separation dynamics. In a usual binary-liquid mixture, the low viscosity makes the phase separation so rapid that within a very short time the phase separation enters in very late stage where gravity plays a significant role. Furthermore, the phase-separation behavior is very sensitive to small temperature changes, and very delicate experiments are required. In a polymer mixture, on the other hand, the high viscosity makes the phase separation very slow. Although it is suitable for studying the initial stage of spinodal decom-

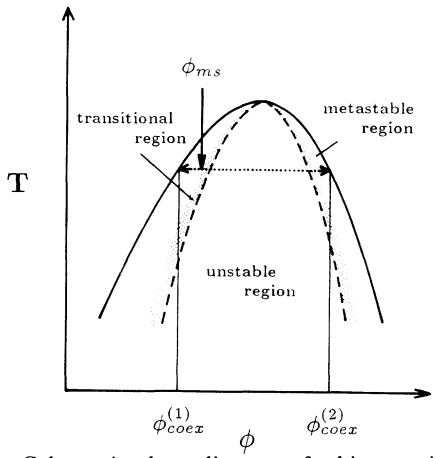

FIG. 1. Schematic phase diagram of a binary mixture. The solid curve is the binodal line (the coexistence curve) and the dashed curve the classical spinodal line. The shaded area is a transitional region from metastability to instability. The broadness of the transition depends on the interaction range. The arrow indicates an off-critical quench condition.

position, it takes too long a time to study nucleation in the metastable state or the overall phase-separation dynamics.

The samples used were mixtures of styrene oligomer (OS) and ϵ-caprolactone oligomer (OCL). The weight-averaged molecular weight M_w of OS was 1000 and that of OCL 5000. M_w/M_n (M_n is the number-averaged molecular weight) of OS was 1.1 and that of OCL 1.4. Figure 1 shows the schematic phase diagram of the mixture. The critical temperature was 156 °C, and the critical composition was 80 wt% OS. We have changed the quench depth ΔT ($=T_{coex}-T$, T_{coex} is the temperature of the binodal line) systematically at a fixed concentration (ϕ_{ms}) under an off-critical condition as shown by the arrow in Fig. 1. The experiments presented in this Letter were carried out in an OCL/OS (65/35) mixture whose T_{coex} was 150.0 °C. The temperature was quenched from 151.0 °C to various temperatures below T_{coex}. The temperature of the sample was controlled within an accuracy of ± 0.1 °C and quenched by using a hot stage (Linkam TH-600). The quench rate was 90 °C/min. The temperature settled within a few seconds after the quench. The pattern-formation process was observed with phase-contrast microscopy. The phase-separated pattern has been quantitatively analyzed by a digital-image-analysis (DIA) method.[17-21]

The typical patterns observed in the NG-type phase-separation process at 145 °C are shown in Fig. 2, while those in the SD-type phase-separation process at 139 °C are shown in Fig. 3. These figures demonstrate the difference in morphology and dynamics between NG and SD, although both have droplet patterns. In NG the nuclei, which look black, were born and grew almost independently. The density of droplets in NG is much lower than in SD. In SD the spatial concentration fluctuations grew in both amplitude and size, and formed droplets which look gray in the photographs. The droplets became darker and darker with time, and became larger and larger mainly by a coalescence mechanism. The droplet-type growth in SD is a result of an off-critical quench or an asymmetric composition. The droplet-type pattern observed in SD is completely different from the percolated-cluster or interconnected pattern observed in the initial or intermediate stage under a critical quench condition.[1,2,19]

In addition to the direct morphological observation, the concentration distribution function $P(\phi)$ clearly shows the difference in phase-separation mechanism between NG and SD. $P(\phi)$ can be directly calculated by a numerical operation of DIA.[19] Figures 4(a) and 4(b) show the temporal change in $P(\phi,t)$ for NG and SD, respectively. In NG, a small peak appears almost at the final equilibrium composition $\phi_{coex}^{(2)}$ and grows without changing its peak position significantly. The main peak around $\phi_{coex}^{(1)}$ does not change much because the volume fraction of the minority phase is so small. This behavior is quite consistent with the general picture of nucleation. In SD, on the other hand, the peak initially becomes broad, reflecting the growth of concentration fluctuations, and starts to deviate from the Gaussian shape because of nonlinearity.[19,20] The $P(\phi)$ becomes bimodal and the amplitude of the concentration fluctuations ($\Delta\phi$) increases with time. Finally, two peaks approach the final concentrations, $\phi_{coex}^{(1)}$ and $\phi_{coex}^{(2)}$. The above behavior of $P(\phi)$ is consistent with the prediction for spinodal decomposition. We can clearly distinguish the type of phase separation, namely, whether the phase separation is NG or SD, from the behavior of $P(\phi,t)$.

Next we show the transition in kinetics from NG to SD with the quench depth (ΔT). We focus our attention on the time evolution of the scattering function $S(k)$ (k is the wave number), which is the one-dimensional (1D)

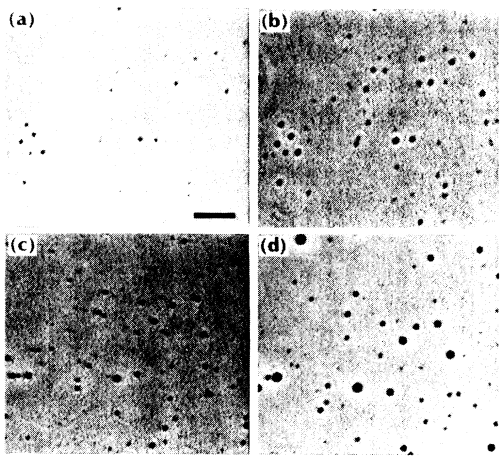

FIG. 2. Temporal change in the patterns observed at 145 °C with optical microscopy during the NG-type phase-separation process. (a)–(d) correspond to the structures at 5, 17, 95, and 1175 s after the quench, respectively. The bar corresponds to 20 μm.

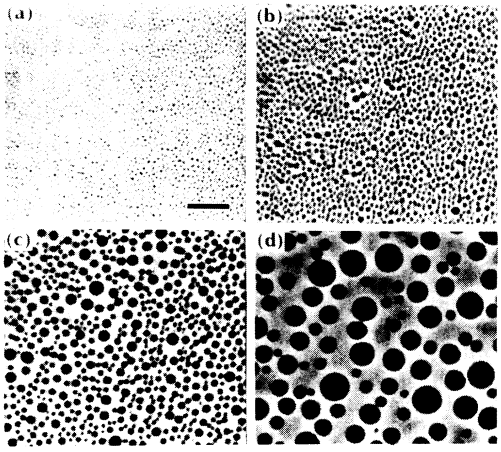

FIG. 3. Temporal change in the patterns observed at 139 °C with optical microscopy during the SD-type phase-separation process. (a)–(d) correspond to the structures at 1, 21, 111, and 6300 s after the quench, respectively. The bar corresponds to 20 μm.

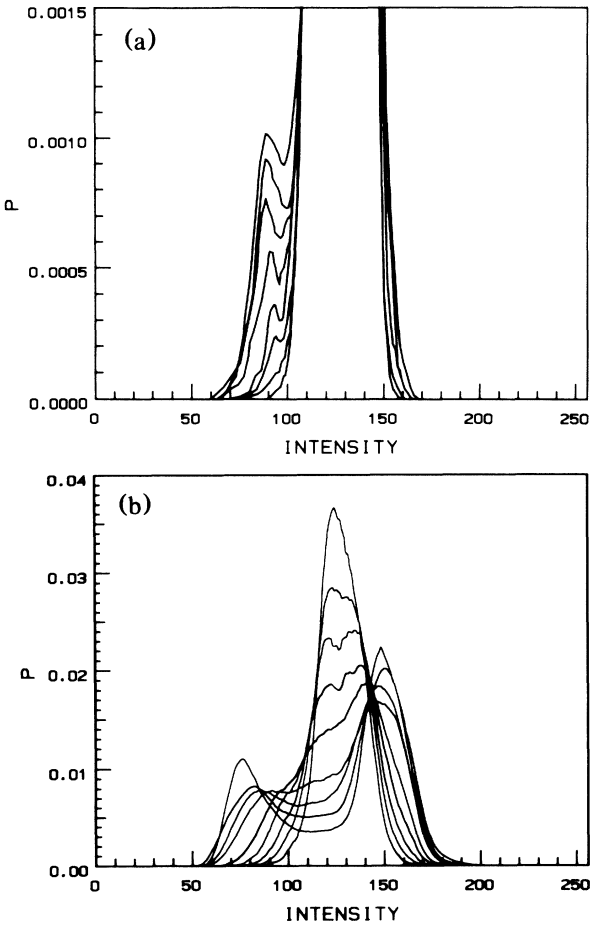

FIG. 4. (a) Temporal change in the concentration distribution function $P(\phi,t)$ for NG observed at 145 °C. Curves correspond to $P(\phi)$ at 1, 13, 95, 395, 1775, 5075, 7200, and 10800 s after quench, respectively, from the bottom to the top around the intensity of 90. Intensity (x axis) corresponds to concentration or composition, ϕ. The scale of the y axis is expanded to show a growing small peak around $\phi_{\rm coex}^{(2)}$. (b) Temporal change in the concentration distribution function $P(\phi,t)$ for SD observed at 139 °C. Curves correspond to $P(\phi)$ at 1, 3, 7, 16, 31, 81, 171, 381, and 1521 s after quench, respectively, from the top to the bottom at the intensity of 128.

radial function obtained from the two-dimensional (2D) power spectrum $P(\mathbf{k})$ of a digitized image.[17] Figure 5 shows the quench-depth dependences of the scattering peak intensity $S(k_{\rm max}(t_1),t_1)$ at a phase-separation time t_1 and the exponent α for the characteristic wavelength $\lambda_{\rm max}$ [$=2\pi/k_{\rm max}$, where $k_{\rm max}$ gives the maximum of $S(k)$]. Even for NG, where nuclei appear almost randomly in space, $S(k)$ has a weak, but distinct peak reflecting both intraparticle and interparticle correlations. $\lambda_{\rm max}$ is found to roughly scale as $t^{-\alpha}$ for all the quench conditions. The values of t_1 chosen here are 100 and 1000 s. For any value of t_1 ($\gtrsim$100 s), $S(k_{\rm max}(t_1),t_1)$ depends on ΔT qualitatively in the same way. Figure 5 clearly shows a clear, but diffuse transition in kinetics between the metastable and unstable re-

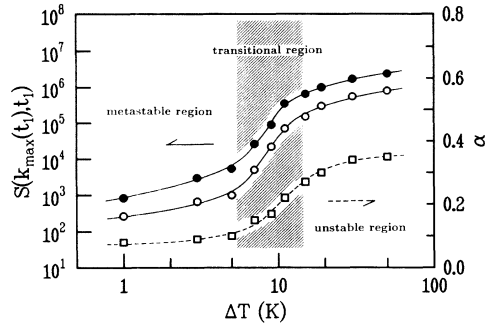

FIG. 5. Dependences of the scattering peak intensity $S(k_{\rm max}(t_1),t_1)$ and the exponent α for the characteristic wavelength $\lambda_{\rm max}$ on the quench depth ΔT. (○, ●) $S(k_{\rm max}(t_1),t_1)$ at the phase-separation time $t_1=100$ and 1000 s, respectively; (□) the exponent α.

gions. From the direct morphological observation, the phase-separation behavior looks like NG above 145 °C, while it looks like SD below 139 °C. The dependences of both $S(k_{\rm max}(t_1),t_1)$ and α on ΔT clearly reflect the difference in the type of phase separation between above 145 °C and below 139 °C. The scattering intensity is much lower in NG than in SD if we compare them at the same phase-separation time. This reflects the difference in both kinetics and $\Delta\phi$ in the final equilibrium state ($\phi_{\rm coex}^{(2)}-\phi_{\rm coex}^{(1)}$), which can be estimated from the phase diagram. The phase-separation speed increases with an increase in the quench depth. In particular, it increases sharply around the transition from metastability to instability, namely, around 142 °C.

The transition observed in Fig. 5 can be explained by the transition in the coarse-graining mechanism. Apparently, $\lambda_{\rm max}$ behaves differently as a function of time below 139 °C compared to above 145 °C. In the unstable region below 139 °C, the exponent α is roughly equal to $\frac{1}{3}$, which is characteristic of the intermediate stage of phase separation in a system with conserved order parameter.[1,2] In the metastable region above 145 °C, on the other hand, the exponent is very small ($\sim\frac{1}{10}$), reflecting very slow coarsening. It should be stressed that around the transition the exponent α smoothly changes its value as a function of the quench depth, with a finite width of several degrees. This is strong evidence that the transition is diffuse and the behavior cannot be explained by the mean-field picture. The problem will be discussed later. The difference in the exponent between NG and SD can be attributed to that in the growth mechanism of droplets. In NG, droplets with almost final composition grow monotonously and almost independently of each other, since a small final volume fraction of the minority phase in NG weakens the interaction between droplets and the collision between droplets is very rare. Therefore, the number of droplets increases roughly at the rate of nucleation except for the late stage. In SD, on the other hand, the initial wavelength of concentration fluctuations is small and the

number density of droplets whose composition is far from the equilibrium value is initially very large. Because of the high density of droplets, droplets often collide with each other and grow efficiently by the coalescence mechanism. The number of droplets decreases monotonously with time[22] as $N \sim t^{-1}$.

As can be seen in Fig. 5, there is a clear, but diffuse transition in kinetics. Here we mention morphological evidence for the broadness of the metastable-unstable transition. At 143 and 141 °C the phase separation initially proceeds in the NG-like manner and a small number of black droplets with high contrast appeared just after the quench. Then many small droplets with low contrast appeared and grew with increasing contrast. This behavior is characteristic of the SD-type phase separation. They grew to a size observable with microscopy at about 18 and 9 s after the quench to 143 and 141 °C, respectively. In other words, NG and SD proceed simultaneously in the transitional region, suggesting that both processes can be thermally activated. The transitional region ranges roughly from 144 to 140 °C. The mixed appearance of the two types of phase separation (NG and SD) indicates the existence of a crossover region between the metastable and unstable regions. This morphological transition coincides very well with the kinetic transition shown in Fig. 5.

In conclusion, we have found a clear, but diffuse transition from metastability to instability from both morphological and kinetic viewpoints. Furthermore, DIA is found to be a powerful tool to clarify the interplay between the geometrical characteristics of the growing objects and the dynamical growth laws. The broad transition probably reflects the fact that for the short-range-force system the barrier for nucleation in the metastable state gradually disappears with an increase in the quench depth, and near the transition infinitesimal fluctuations may not be necessarily unstable because of nonlinearity and the short-range nature of the interaction even in the unstable region. It is reasonable to believe that our system is a short-range-force system since the molecular weights of the oligomers are not large enough to cause a long-range interaction and the entanglement effect. It should be mentioned that polydispersity may also make the transition diffuse, although our samples have rather narrow distributions of molecular weight. Since in the mean-field theory or the long-range-force limit the spinodal is defined as a sharp line even in polydisperse polymer mixtures,[23] polydispersity does not affect our main conclusion that the diffuse transition observed is due to a short-range nature of the interaction. However, it may affect the degree of broadness of the transition. It would be very meaningful to study the molecular-weight dependence of the width of the transition. This kind of systematic control of the interaction range may be possible only in oligomer or polymer mixtures.

The initial number of droplets rapidly increases with a decrease in the barrier for nucleation. When this energy barrier becomes very small (of the order of $k_B T$), a high density of unstable fluctuations develops. Both morphology and kinetics of phase separation drastically change at the transition from metastability to instability, although the transition is not so sharp. This indicates a sudden increase in the droplet density at the transition with the quench depth. The change in droplet density also affects the coarsening process. With an increase in the quench depth, droplets start to interact with each other even in the initial stage beyond a certain threshold of droplet density, since conservation of concentration causes an interaction between droplets through the depletion effect. This causes the change in the main droplet-growth mechanism from independent growth to coalescence, and strongly affects the coarse-graining dynamics. The details on the coarsening process and the difference in the type of spatial point-distribution pattern between NG and SD will be discussed elsewhere.

[1]J. D. Gunton, M. San Miguel, and P. Sahni, in *Phase Transition and Critical Phenomena,* edited by C. Domb and J. H. Lebowitz (Academic, London, 1983), Vol. 8.

[2]*Dynamics of Ordering Processes in Condensed Matter,* edited by S. Komura and H. Furukawa (Plenum, New York, 1987).

[3]J. S. Langer, Physica (Utrecht) **73**, 61 (1974).

[4]K. Binder, Phys. Rev. A **29**, 341 (1984).

[5]K. Binder, Physica (Amsterdam) **140A**, 35 (1986).

[6]D. W. Herrmann, W. Klein, and D. Stauffer, Phys. Rev. Lett. **49**, 1262 (1982).

[7]K. Kaski, K. Binder, and J. D. Gunton, Phys. Rev. B **29**, 3996 (1984).

[8]W. Klein and C. Unger, Phys. Rev. B **28**, 445 (1983).

[9]C. Unger and W. Klein, Phys. Rev. B **29**, 2698 (1984).

[10]J. S. Huang, S. Vernon, and N. C. Wong, Phys. Rev. Lett. **33**, 140 (1974).

[11]J. S. Huang, W. I. Goldburg, and M. R. Moldover, Phys. Rev. Lett. **34**, 639 (1975).

[12]A. J. Schwartz, S. Krishnamurthy, and W. I. Goldburg, Phys. Rev. A **21**, 1331 (1980).

[13]G. C. Howland, N. C. Wang, and C. M. Knobler, J. Chem. Phys. **73**, 522 (1980).

[14]S. Krishnamurthy and W. I. Goldburg, Phys. Rev. A **22**, 2147 (1980).

[15]S. Krishnamurthy and R. Bansil, Phys. Rev. Lett. **50**, 2010 (1983).

[16]E. D. Siebert and C. M. Knobler, Phys. Rev. Lett. **52**, 1133 (1984).

[17]H. Tanaka, T. Hayashi, and T. Nishi, J. Appl. Phys. **59**, 3627 (1986).

[18]H. Tanaka, T. Hayashi, and T. Nishi, J. Appl. Phys. **65**, 4480 (1989).

[19]H. Tanaka and T. Nishi, Phys. Rev. Lett. **59**, 692 (1987).

[20]H. Tanaka and T. Nishi, Jpn. J. Appl. Phys. **27**, 1783 (1988).

[21]H. Tanaka and T. Nishi, Jpn. J. Appl. Phys. **27**, 1787 (1988).

[22]H. Tanaka, T. Hayashi, and T. Nishi (to be published).

[23]R. Koningsveld and H. A. G. Chermin, Proc. Roy. Soc. London A **319**, 331 (1970).

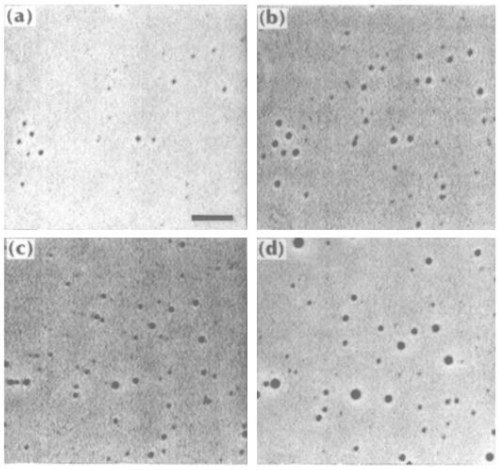

FIG. 2. Temporal change in the patterns observed at 145 °C with optical microscopy during the NG-type phase-separation process. (a)–(d) correspond to the structures at 5, 17, 95, and 1175 s after the quench, respectively. The bar corresponds to 20 μm.

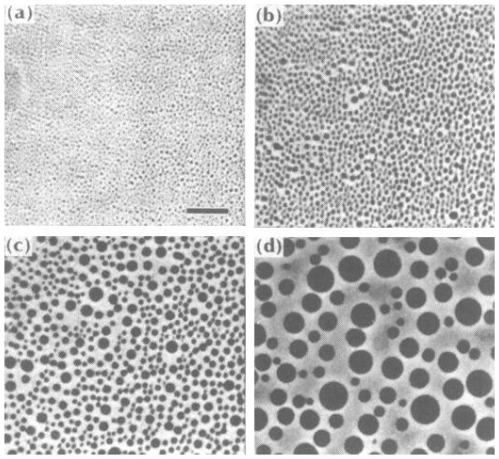

FIG. 3. Temporal change in the patterns observed at 139 °C with optical microscopy during the SD-type phase-separation process. (a)–(d) correspond to the structures at 1, 21, 111, and 6300 s after the quench, respectively. The bar corresponds to 20 μm.